

# Artificial neural network simulations and experimental results: Removal of trichlorophenol from water using *Chromolaena odorata* stem

Derrick S Dlamini<sup>1</sup>, Ajay K Mishra<sup>1</sup> and Bhekie B Mamba<sup>1\*</sup>

<sup>1</sup>Department of Applied Chemistry, University of Johannesburg, PO Box 17011, Doornfontein 2028, Johannesburg, Gauteng, South Africa

## ABSTRACT

A novel adsorbent for trichlorophenol (TCP) has been developed through the treatment of *Chromolaena odorata* (Odorata) with iodated table salt. Odorata is an abundant and problematic alien plant which we have found to be effective in removing TCP from aqueous solutions. Kinetic batch tests demonstrated that at pH 5, 99% of TCP could be removed from a solution given sufficient adsorbent loading rate and adsorption contact time with Odorata treated with table salt. Adsorption data were found to fit a 2-layer feed-forward artificial neural network (ANN) with 10 neurons using the Levenberg-Marquardt (trainlm) algorithm. The ability of Odorata to extract TCP from water was tested using equilibrium, kinetic and thermodynamic studies. Thermodynamic studies showed that the adsorption of TCP by the new adsorbent is thermally feasible and is governed by a chemical adsorption mechanism. It was established that the experimental data fit the selected adsorption isotherms in the following order: Langmuir > Freundlich > Temkin > Dubinin-Radushkevich (D-R). Kinetic modelling was done using intra-particle diffusion, liquid-film, pseudo-first order and pseudo-second order models. With the aid of the normalised standard deviation, the pseudo-second order was found to be the appropriate rate expression for the adsorption data. Liquid-film diffusion was the rate-determining stage of the adsorption process.

**Keywords:** *Chromolaena odorata*; TCP; adsorption; table salt; ANN

## INTRODUCTION

The pollution of water by organic materials is inexorable. Trichlorophenol (TCP) is one of the problematic compounds that end up in water as a result of industrial and agricultural activities. The main pollution sources containing chlorinated phenols like TCP are the wastewaters from pesticide, paint, solvent, pharmaceuticals, wood, paper and pulp industries as well as water-disinfecting process (Hameed et al., 2008). Removing TCP from water is crucial. TCP is highly toxic, carcinogenic, structurally stable and persistent in the environment (Hameed et al., 2008). According to Tan et al. (2009) the stable C-Cl bond and the position of chlorine atoms relative to the hydroxyl group are responsible for TCP's toxicity and persistence in the biological environment.

Unlike inorganic water pollutants (like heavy metals), the concentration of organic compounds like TCP in water can be reduced by photo-degradation. Another technique used for the removal of TCP from aqueous media is membrane filtration technology. The major disadvantages of the membrane processes are the costs, as membrane filtration processes use pressure and their lifetime is limited before fouling (Subramani et al., 2009; Hoek et al., 2011). In accordance with the abundant literature data (Pei et al., 2007; Fan et al., 2011; Puyol et al., 2011; Zaghoulane-Boudiaf et al., 2011), adsorption is one of the most popular techniques for the uptake of TCP from water. In recent years, a lot of attention has focused on developing effective adsorbents which are able to remove the pollutants from

the contaminated wastewater at low cost. Cost is actually an important parameter for comparing the suitability of adsorbent materials. According to Ahmaruzzaman (2008), an adsorbent can be categorised as low-cost if it requires little processing and is abundant in nature.

Most of the adsorbents that have been developed can be loosely classified as either inorganic or agricultural. One inorganic adsorbent that has been widely studied is clay. For example, Dlamini et al. used organo-montmorillonite (2012a) and Bentonite (2012b; 2012c) as filler in polymeric composites aimed at removing lead ions from water. Motsa et al. (2011) and Mthombo et al. (2011) used clinoptilolite as a filler material in the preparation of composites which were used for the removal of heavy metals from water. Such adsorbents (polymeric composites) are ideal for easy recovery and are stable in the water environment especially if the polymer used as a support is hydrophobic. The downside with composite adsorbents is that a lot of the filler needs to be used, while lower adsorption efficiency is recorded compared to powder adsorbents. The agricultural products that have been used as adsorbents for heavy metals and organic pollutants are *Acacia leucocephala* bark (Kumar et al., 2012), rice husk (Mahvi et al., 2004), sawdust (Shukla et al., 2002) and TiO<sub>2</sub> (Dutta et al., 2010), to mention but a few.

Agricultural adsorbents are also called biosorbents. These materials contain various organic compounds (lignin, cellulose and hemicellulose) with polyphenolic groups that might be useful for binding TCP through different mechanisms. Agricultural products have to undergo treatment before they can be used in water treatment to remove lignin-based colour materials. To this end, NaOH (Mthombo et al., (2011), KCl and NaCl have been commonly used for preparing biosorbents; however, for this study the iodated salt has been used.

\* To whom all correspondence should be addressed.

+27 11-559-6516; fax: +27 11-559-6425;

e-mail: [bmamba@uj.ac.za](mailto:bmamba@uj.ac.za)

Received 22 November 2012; accepted in revised form 28 January 2014.

In the present study, we explored the potential application of *Chromolaena odorata* (forthwith referred to as Odorata) treated using iodated table salt as a biosorbent for TCP in water. To the best of our knowledge no study has previously been reported on the use of Odorata treated with table salt as an adsorbent for TCP, or even the application of Odorata as an adsorbent. Odorata is a problematic alien plant that affects agricultural activities. This study is important because the processing of Odorata is cheap and it is abundantly available especially in Southern Africa, a region under clean-water stress. The utilisation of table salt treated–Odorata could solve the problem of access to cheaper material for adsorption in water pollutant control systems in the rural areas, especially in Third World countries.

Solving complex problems is a challenge and one efficient way of finding a solution is applying the ‘divide and conquer’ principle. This principle requires that a complex system be decomposed into simpler elements in order to be able to understand it. Neural networks are one way to achieving this. There are many levels of abstraction when it comes to the subject of artificial neural networks (ANN) in relation to neuroscience; therefore there is no simple definition of ANN. An artificial neuron is a computational model inspired by the natural biological neurons in the brain. In the present study, a 2-layer ANN model using a feed-forward propagation algorithm for modelling TCP adsorption by Odorata was designed. An optimisation study to determine the optimal number of neurons and transfer functions was done. A computer-simulated model like ANN is necessary in developing an automated wastewater treatment plant to reduce the operating cost of the plant.

## MATERIALS AND METHODS

### Materials

Odorata stems were collected at a non-agricultural area, Matsapha, Swaziland. The plant was collected at a non-agricultural area to avoid the presence of toxic soluble leachate, which could possibly emanate from pesticides. Iodated table salt was purchased at a supermarket at Campus Square, Johannesburg, South Africa. Trichlorophenol (TCP), NaOH and HCl were procured from Sigma Aldrich, Johannesburg, South Africa.

### Adsorbent preparation

Odorata stems were chopped into small pieces of about 2 cm and then left to dry in open air for 8 months. Bark was stripped off and the dry stems were powdered and sieved to  $\leq 38 \mu\text{m}$  particles using a laboratory test sieve with a pore size of  $38 \mu\text{m}$ . Moisture was removed from the micro-particles by using an oven programmed to  $100^\circ\text{C}$  for 24 h. The micro-particles were then soaked in a solution of 0.5 M iodated table salt. The solution was changed 3 times in 3 days. After that, the material was rinsed with deionised water until the filtrate had a pH of 7 and then dried again in an oven at  $100^\circ\text{C}$  to remove water.

### Fourier transform infrared (FTIR) spectroscopy

The functional properties were measured directly by Bruker Tensor 27 Fourier transform infrared (FTIR) spectrometer equipped with diamond/ZnSe universal germanium-attenuated total reflectance (ATR). 10 scans were collected per sample at a resolution of  $4 \text{ cm}^{-1}$ .

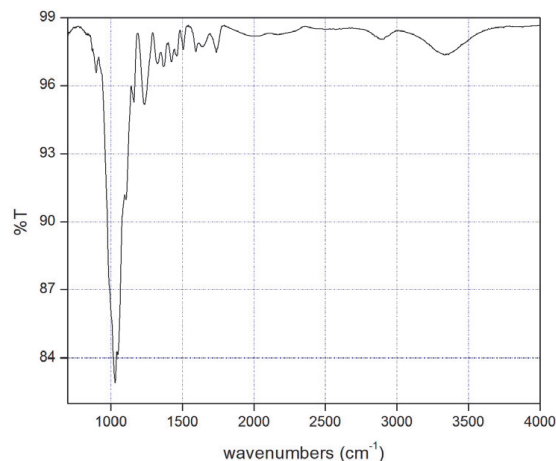


**Figure 1**  
FT-IR spectrum of Odorata treated with iodated table salt

### Batch adsorption studies

The adsorptive properties of the table salt treated–Odorata were tested for the removal of TCP from aqueous media. To minimise the losses of TCP by both photochemical decomposition and volatilisation, the experiments were carried out in brown bottles. The effect of pH, contact time, temperature, and initial concentration was investigated using an adsorbent dose of  $10 \text{ g}\cdot\text{L}^{-1}$ . The pH was adjusted by using 0.1 M HCl and 0.1 M NaOH. The remaining concentration after adsorption was determined by UV spectroscopy (UV-2550, Shimadzu) at a wavelength ( $\lambda$ ) of 296 nm. The pollutant uptake is reported in terms of per cent removal ( $R(\%)$ ):

$$R(\%) = 100 \times \frac{C_o - C_t}{C_o} \quad (1)$$

where:

$C_o$  and  $C_t$  are the initial concentration and the concentration at time  $t$ , respectively

### Definition of the ANN model

In this study, the training, validation and testing of the ANN model was carried out using NN tool box™ on MATLAB 7.11.0 (R2010b) mathematical software. A two-layer feed-forward neural network using tansig and purelin transfer functions in the input and output layer, respectively, was employed to simulate the adsorption of TCP by the Odorata. The adsorption efficiency was used as the output.

## RESULTS AND DISCUSSION

### FTIR analyses

The FTIR results for the Odorata powder are shown in Fig. 1. Hypothetically, plant fibre materials contain chiefly cellulose and lignin. The spectra shows a weak broad peak at  $3335 \text{ cm}^{-1}$ . This band can be assigned to free hydroxyl groups of cellulose (Szopa et al., 2009).

The band at  $1738 \text{ cm}^{-1}$  and  $1424 \text{ cm}^{-1}$  represents  $-\text{COOH}$  groups, probably from pectins, and  $-\text{CH}_2$  bending of cellulose, respectively (Alix et al., 2009). Another peak representing  $-\text{COOH}$  occurs at  $1594 \text{ cm}^{-1}$ , suggesting the presence of lignin (Alix et al., 2009), as confirmed by the band at  $667 \text{ cm}^{-1}$ . The

	Learning algorithm				
	trainlm	trainbfg	trainoss	traincgb	traincgf
<b>R<sup>2</sup></b>					
Train	1	0.9383	0.8889	0.9897	0.988
Validation	0.9998	0.9078	0.8997	0.9823	0.981
Test	0.9994	0.9183	0.8898	0.9906	0.9844
Total	0.9999	0.9194	0.8591	0.9971	0.9881
<b>MSE</b>					
Total	0.3087	11.25	22.1	2.433	4.087

broad and strong band at 1 032 cm<sup>-1</sup> can be attributed to the C-O stretching vibration of the cellulose backbone (Alix et al., 2009). The oxygen atoms in the Odorata should play a big role in the adsorption of TCP from water. The -COOH, -OH, and C-O terminals should play a huge role in the removal of TCP from water.

## ANN design

### Selection of training algorithm

The learning algorithm is another parameter that deserves attention because different learning algorithms can produce a network with different accuracies towards specific data. The Levenberg-Marquardt (*trainlm*), Powell-Beale Restarts (*traincgb*), Fletcher-Reeves Update (*traincgf*), and Quasi-Newton (*trainbfg*, *trainoss*) learning algorithms were tested through trial-and-error to discover the best performing algorithm for the data used in this study. The best algorithm was selected based on regression ( $R^2$ ) value and MSE. The results are summarised in Table 1.

A good training algorithm should have a high  $R^2$  but a small MSE. The *trainlm* learning algorithm had the highest  $R^2$  values, ranging from 0.9994 to 1.000, and *trainoss* algorithm had the lowest values. These results clearly indicate that *trainlm* is the best training system for the data used in this study. Turana et al. (2011) found *trainlm* to be the optimum learning algorithm in modelling the biosorption of Zn(II) from leachate.

### Optimising network architecture

The network design was optimised in terms of the number of neurons. The suitable number of neurons was selected based on the lowest MSE. The results of the effect of the number of neurons in the modelling of the adsorption of TCP by Odorata are illustrated in Fig. 2.

From Fig. 2, the MSE initially decreases with an increase in the number of neurons and increases thereafter. A parallel observation was reported by Yetilmezsoy et al. (2008) for a study modelling Pb(II) adsorption from aqueous environment by Antep pistachio shells. In the present study, the lowest MSE is 0.3489, corresponding to 10 neurons. The increment at higher neuron numbers can be ascribed to the characteristics of the MSE performance index and the input vector used (Yetilmezsoy et al., 2008). Based on these results, 10 neurons in the hidden layer were considered optimal for the modelling of TCP adsorption by Odorata treated with table salt.

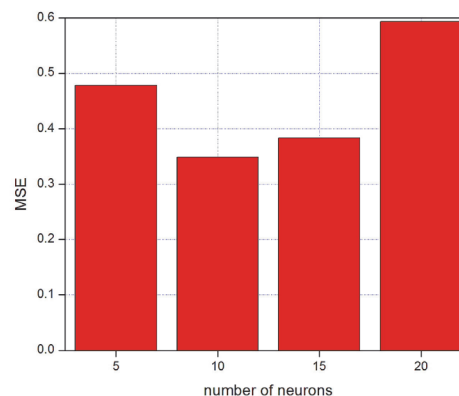


Figure 2  
Effect of the number of neurons

## Trichlorophenol adsorption and ANN application

### Effect of initial concentration and agitation time

The results illustrating how the adsorption of TCP by the Odorata changed with time and initial concentration are shown in Fig. 3. The results are presented in terms of adsorption efficiency.

Based on these results, the plots can be divided into 3 stages. The first stage occurs in the initial 30 min of the experiment. In this stage, the adsorption happens faster because of the abundant available adsorption sites. In the second stage the amount of TCP adsorbed onto the Odorata is approaching a state of dynamic equilibrium with the amount of TCP desorbed from the Odorata. The adsorption time profile has a lower slope at this stage than in the first stage. The third stage can be distinguished by the constant adsorption efficiency as a result of saturation. The contact time of equilibrium was found to be 60 min, after which no more TCP was removed from solution. The 60-min equilibrium contact time is interesting because equilibrium time is one of the important parameters for economical wastewater treatment applications (Denizli et al., 2005). Denizli et al. (2005) reported an equilibrium time of 240 min in a study using dead fungus *Pleurotus sajor caju* as an adsorbent for TCP. Zaghouane-Boudiaf et al. (2011) investigated the adsorption of TCP using organo-montmorillonite and reported an equilibrium contact time of 30 min.

The initial concentration of TCP was varied from 50 to 100 mg·l<sup>-1</sup>. At an initial concentration of 50 mg·l<sup>-1</sup>, the equilibrium adsorption efficiency was found to be 99%. When the concentration was increased to 65 mg·l<sup>-1</sup>, the equilibrium adsorption efficiency slightly decreased to 94%. In the initial concentration range used here, the lowest per cent adsorption (88%) was recorded at an initial concentration of 100 mg·l<sup>-1</sup>. These adsorption efficiencies suggest that the Odorata could be useful in TCP removal from water. The fibre derives adsorption properties from its capability for hydrogen bonding, Van der Waals' interactions or hydrophobic bonding arising from either strong or weak interactions. Plant material generally possesses crystalline and amorphous regions in the cellulose structure. The amorphous region can absorb dyes easily. The hydrophilic hydroxyl groups present in the amorphous region can chemically interact with suitable functional groups of the target pollutant. However, the crystalline region is impermeable and this character can be eliminated by chemical modification.

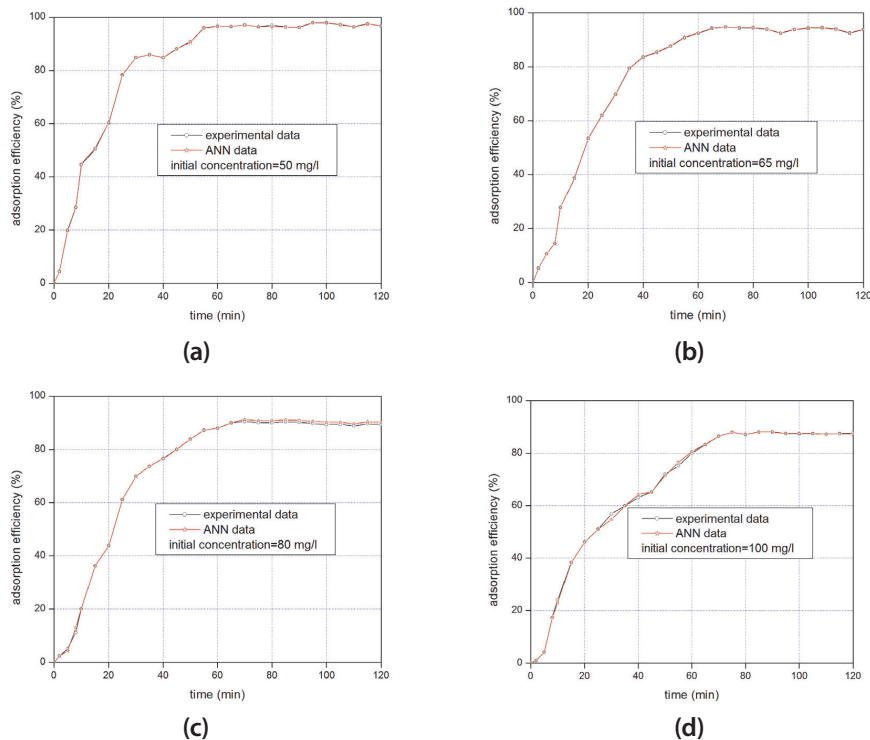


**Figure 3**  
Effect of initial concentration at pH 5

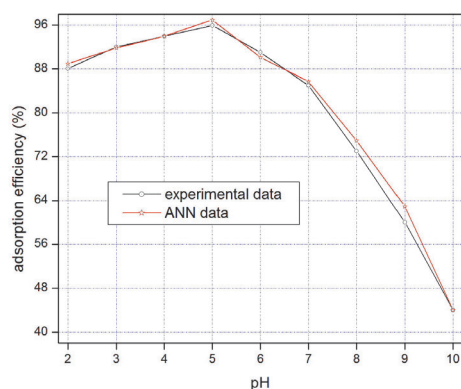


**Figure 4**  
Effect of pH on the adsorption of TCP

The time profile for each initial concentration was simulated using the 2-layer feed-forward ANN. It can be seen in Fig. 3 that the simulated adsorption efficiency was generally close to the experimental per cent TCP adsorption. The standard deviation was calculated using the real adsorption and simulated data and was plotted against time (see Appendix: Fig. S1). The standard deviation ranged from 0 to 1.5 with more data densely clustered below 0.25, indicating that there is indeed a close correlation between the experimental and ANN data.

#### Effect of pH on the adsorption efficiency

Solution pH is one of the most fundamental parameters for adsorption because it determines the interaction in the water-adsorbent interface. The effect of pH on the adsorption of TCP onto *Odorata* is shown in Fig. 4 in terms of per cent adsorption.

From Fig. 4, the adsorption initially increased gradually with an increase in pH until pH 5, and then decreased aggressively thereafter with an increase in pH. Hydrogen bonding

of the phenolic hydroxyl and chloride groups in TCP with the oxygen sites on the surface of *Odorata* is the most likely mechanism for adsorption. The adsorption may not be exclusively due to the phenolic hydroxyl and chloride groups; physical adsorption is also possible. At lower pH there would be hydronium ions on the surface of the adsorbent and the TCP would be positively charged due to hydration. The charges on the TCP and *Odorata* would cause repulsion between the two species; hence the observed trend between pH 2 and 5. As the pH of the solution increases, there would be a decrease in the hydronium ions and the concentration of hydroxide ions would be augmented. At higher pH, TCP is partially ionised (Fan et al., 2011) while the functional groups of *Odorata* are either neutral or negatively charged (Kumar et al., 2012). Therefore, the decrease in the adsorption efficiency above pH 5 can be attributed to repulsions between the TCP and the *Odorata*. Moreover, the partially ionised TCP is highly soluble in water and forms strong phenolate-water bonds thereby 'blocking' the adsorbate from interacting with the adsorbent. A similar trend in the change of TCP adsorption as a function of pH was reported by Kumar et al. (2012) in the uptake of 2,4,6-trichlorophenol from aqueous solutions by *Acacia leucocephala* bark. Based on the results in Fig. 4, pH 5 is the optimum pH for the removal of TCP from water by *Odorata*. Thus, the adsorption of TCP can be controlled by changing the pH. It is worth noting that the NN data curve is identical to the experimental data curve.

#### Effect of temperature on the adsorption efficiency

The effect of temperature on the removal of TCP from water using *Odorata* was investigated at a temperature range of 293–323 K. The results are shown in Fig. 5. The adsorption efficiency increased with an increase in temperature. Tan et al. (2009) reported a similar observation in a study on the removal of 2,4,6-trichlorophenol from water using oil palm empty fruit bunch based activated carbon at a temperature range of 303–323 K.



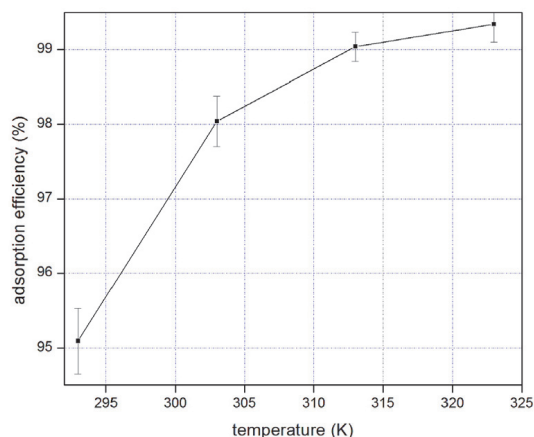


**Figure 5**  
Effect of temperature on the adsorption of TCP at pH 5

The observed increase in TCP removal from water by the Odorata can be attributed to an increase in the TCP mobility with an increase in temperature. To gain deeper insight into the effect of temperature on the uptake of TCP by the Odorata, the thermodynamic feasibility of the study was determined using the thermodynamic parameters: free Gibbs energy ( $\Delta G^0$ ), enthalpy ( $\Delta H^0$ ), and entropy ( $\Delta S^0$ ).  $\Delta G^0$  was computed using the following relation:

$$\Delta G^0 = -RT \ln K_c \quad (2)$$

where:

$R$  is the gas constant ( $8.314 \text{ J}\cdot\text{mol}^{-1}\cdot\text{K}^{-1}$ )

$T$  is temperature (K)

$K_c$  is the apparent equilibrium constant ( $K_c$ ) of the adsorption and is defined in terms of the TCP adsorbed at equilibrium ( $C_{ads}$ ) and the equilibrium TCP concentration ( $C_e$ ), as per the following equation (Sölener et al., 2008):

$$K_c = \frac{C_{ads}}{C_e} \quad (3)$$

The values of  $\Delta H^0$  and  $\Delta S^0$  were calculated from the slope and intercept of the plot of  $\ln K_c$  vs. reciprocal of temperature ( $T$ ) (Sölener et al., 2008; Tan et al., 2009).  $K_c$  is related to  $\Delta H^0$  and  $\Delta S^0$  by the following equation:

$$\ln K_c = \frac{\Delta S^0}{R} - \frac{\Delta H^0}{RT} \quad (4)$$

Equation (4) assumes that there is a linear relationship between the  $\ln K_c$  and  $1/T$ . The thermodynamic parameters tabulated using this equation are given in Table 2.

It has been reported that negative values of  $\Delta G^0$  indicate spontaneous adsorption while positive values mean that the adsorption process is non-spontaneous (Shin et al., 2010; Sen et

TABLE 2				
Thermodynamic parameters				
$\Delta G^0$ (kJ·mol <sup>-1</sup> )			$\Delta H^0$ (kJ·mol <sup>-1</sup> )	$\Delta S^0$ (J·mol <sup>-1</sup> ·K)
Temperature (K)				
293	303	313	-63.8	-242.6
-84.09	-107.3	-123.1		

al., 2011). Errais et al. (2011) reported that the negative values of  $\Delta G^0$  indicate that the adsorption process is thermodynamically feasible. Therefore, the adsorption of TCP on Odorata is thermodynamically feasible at the temperature range used in this study. According to Zaghouane-Boudiaf et al. (2011),  $\Delta G^0$  values ranging from 0 to  $-30 \text{ kJ}\cdot\text{mol}^{-1}$  and  $-80$  to  $-400 \text{ kJ}\cdot\text{mol}^{-1}$  indicate physical and chemical adsorption, respectively. The values of  $\Delta G^0$  in Table 2 show that the adsorption of TCP by Odorata occurred through chemical adsorption. This observation was supported by the  $\Delta H^0$  which falls within the range:  $-42$  to  $-125 \text{ kJ}\cdot\text{mol}^{-1}$ .

### Adsorption isotherms

In an attempt to optimise the design of an adsorption system, it is imperative to find the most appropriate correlation for the equilibrium curves (Hameed et al., 2008). Equilibrium results are reported in terms of the amount of TCP adsorbed at equilibrium per unit weight of the adsorbent,  $q_e$  ( $\text{mg}\cdot\text{g}^{-1}$ ), which can be represented as follows:

$$q_e = \frac{(C_o - C_e)v}{w_s} \quad (5)$$

where:

$v$  is the analyte solution volume (l)

$w_s$  is the weight of the adsorbent (g)

Herein, 4 adsorption isotherms: the Langmuir, Freundlich, Dubinin-Radushkevich (D-R) and Temkin were employed to fit the adsorption data of TCP adsorption from water by Odorata. The Langmuir isotherm assumes monolayer adsorption and is expressed as follows:

$$\frac{C_e}{q_e} = \frac{1}{bQ_0} + \frac{C_e}{Q_0} \quad (6)$$

where:

$Q_0$  is the adsorption capacity ( $\text{mg}\cdot\text{g}^{-1}$ )

$b$  is the energy of adsorption ( $\text{l}\cdot\text{mg}^{-1}$ )

If the data fit a Langmuir isotherm, a plot of  $C_e/q_e$  versus  $C_e$  should give a linear plot (results shown in Fig. 6(a)). The essential feature of the Langmuir isotherm is the equilibrium parameter,  $R_L$ , a dimensionless constant that can be presented as follows:

$$R_L = \frac{1}{1 + bC_o} \quad (7)$$

$R_L$  indicates whether the adsorption is unfavourable ( $R_L > 1$ ), linear ( $R_L = 1$ ), favourable ( $0 < R_L < 1$ ) or irreversible ( $R_L = 0$ ) (Sölener et al., 2008). Therefore, the adsorption of TCP onto the Odorata was favourable under conditions used in this study. The Freundlich model is used to describe heterogeneous systems. The isotherm assumes that the adsorbent surface sites have an array of different binding energies. The Freundlich isotherm is presented as follows:

$$\log q_e = \log K_F + \frac{1}{n} \log C_e \quad (8)$$

where:

$q_e$  is the amount adsorbed at equilibrium ( $\text{mg}\cdot\text{g}^{-1}$ )

$C_e$  is the equilibrium concentration of the adsorbate

$K_F$  and  $n$  are the Freundlich constants which can be determined from the linear graph of  $\log q_e$  against  $\log C_e$ . The Freundlich graph is shown in Fig. 6(b).

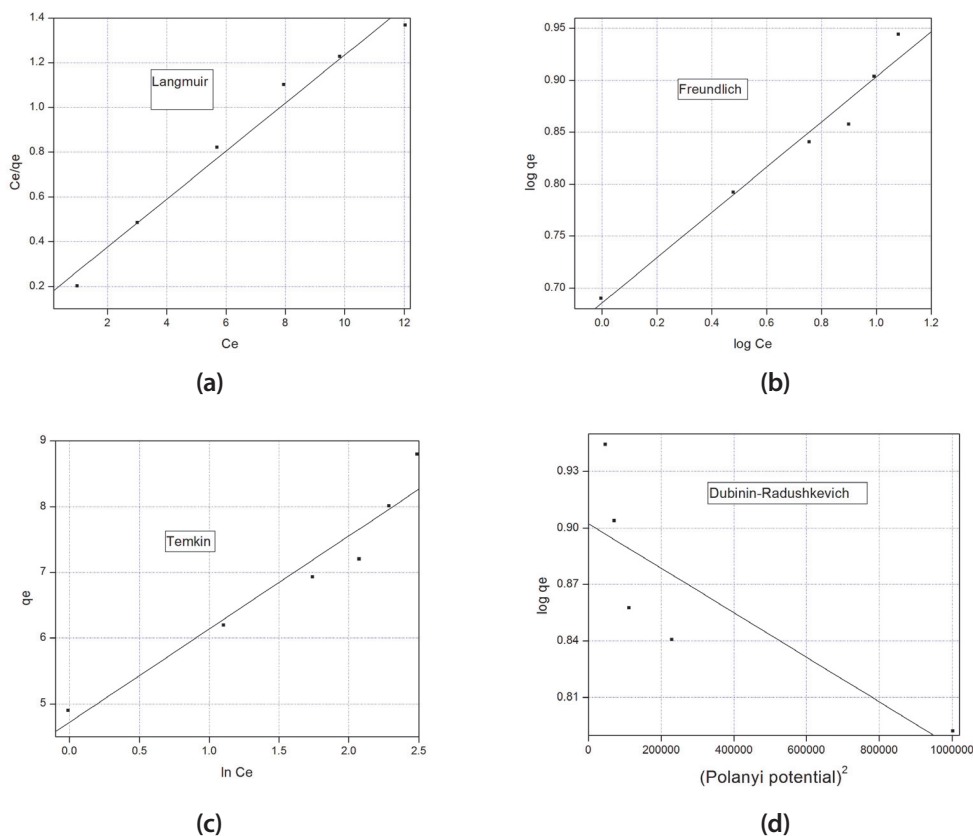


**Figure 6**  
Adsorption isotherms:  
(a) Langmuir;  
(b) Freundlich;  
(c) Temkin, and;  
(d) Dubinin-Radushkevich isotherms

Another isotherm that was used in the present work is the Temkin model. The linear form of the Temkin isotherm is expressed as follows (Kumar et al., 2012):

$$\varepsilon = RT \ln \left[ 1 + \frac{1}{C_e} \right] \quad (9)$$

where:

$RT/b_T = B$  ( $\text{J}\cdot\text{mol}^{-1}$ ) is the Temkin constant related to heat of sorption

$A$  ( $\ell\cdot\text{g}^{-1}$ ) is the equilibrium binding constant corresponding to the maximum binding energy.

The TCP adsorption data was fitted in the Temkin model by plotting  $qe$  vs.  $\ln C_e$  and the results are shown in Fig. 6(c). The D-R model is shown below (Dlamini et al., 2012a):

$$\ln q_e = \ln q_m - K\varepsilon^2 \quad (10)$$

where:

$q_m$  is the theoretical saturation capacity

$\varepsilon$  is the Polanyi potential calculated as follows:

$$q_e = \frac{RT}{b_T} \ln A + \frac{RT}{b_T} \ln C_e \quad (11)$$

A linear plot of  $\ln q_e$  against  $\varepsilon^2$  is accepted as an indication that the data fits the D-R model. The D-R curve is shown in Fig. 6(d).

According to Kara et al. (2008), the constant,  $K$ , is related to the mean free energy of sorption per mole of the sorbate as it is transferred to the surface of the solid from infinite distance in the solution, and this energy can be computed using the following relationship:

$$E = (2K)^{-1/2} \quad (12)$$

TABLE 3			
Adsorption isotherm parameters			
Isotherms	Constants		$R^2$
Langmuir	$Q_o$	$b$	0.9787
	9.311	1.493	
Freundlich	$K_F$	$1/n$	0.9687
	1.985	0.2175	
Tempkin	$A_T$	$b_T$	0.9338
	1.351	1 709	
D-R	$q_m$	$E$	0.6635
	2.654	0.4861	

The parameters tabulated from the 4 isotherms are summarised in Table 3. The correlation coefficients ( $R^2$ ) suggest that the experimental data fit the models in the following order: Langmuir > Freundlich > Temkin > D-R. The Langmuir, Freundlich and Temkin models gave good  $R^2$  (>0.900).

A value of  $1/n$  between 0 and 1 is a measure of surface heterogeneity, becoming more heterogeneous as its value approaches zero (Kumar et al., 2012). From the value of  $1/n$  shown in Table 3, the adsorption of TCP onto Odorata is favourable and occurred in a heterogeneous surface. Heterogeneity in plant fibre adsorbents for molecules like TCP arise from the different atoms (H and O) participating in the adsorption process. The low energy (0.4861 kJ/mol) calculated obtained from the D-R model confirms that the removal of TCP was indeed mostly through dipole-dipole physical adsorption in conjunction with electrostatic adsorption.

## ADSORPTION KINETICS

Adsorption occurs in at least 4 stages that can have different

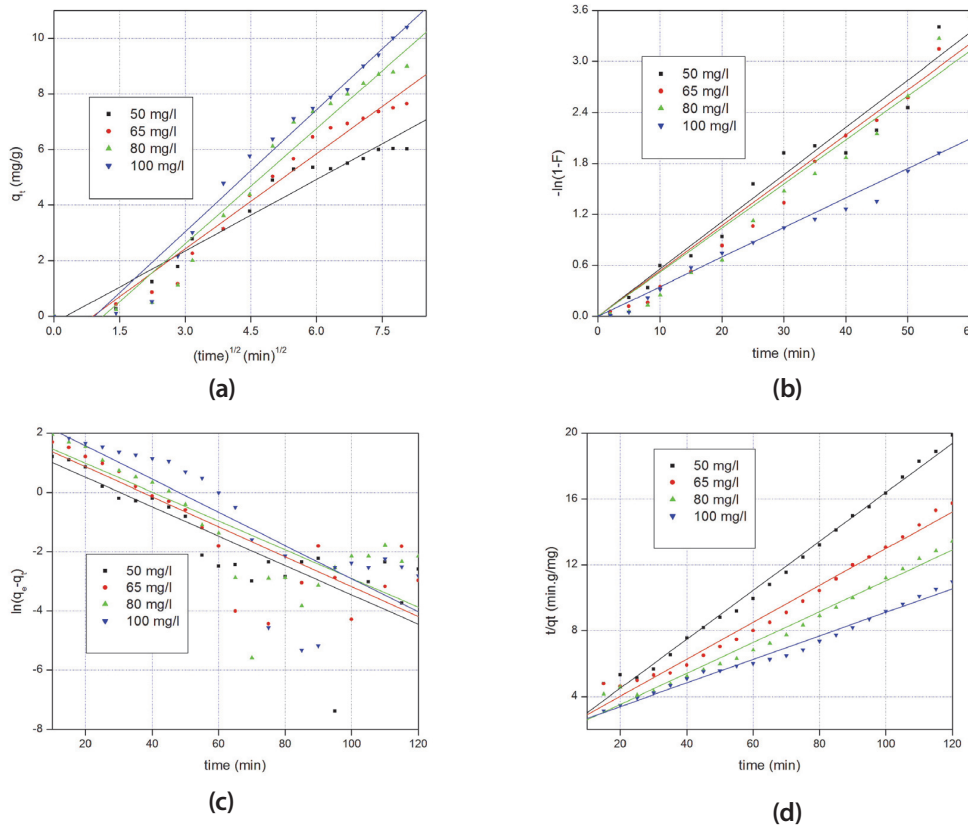


**Figure 7**  
Kinetic models: (a) pseudo-first order; (b) pseudo-second order; (c) intra-particle diffusion, and (d) liquid-film model.

kinetic rates (Bystrzejewski et al., 2011). Firstly, the transport of the analyte will involve the migration of TCP from the bulk liquid to the adsorbent particles. Since the *Odorata* particles would be enveloped by liquid film, the second stage of the adsorption process of TCP involves penetration through the film to gain contact with the adsorbent particles. In the next step, there will be intra-particle diffusion of the TCP into the *Odorata* particles and then adsorption will occur. It is imperative to identify the dominant (slowest) stage because it may control the kinetics of the adsorption process and therefore determine the removal rate of TCP from the aqueous solution.

However, since the adsorption experiments were done under vigorous shaking ( $250 \text{ r}\cdot\text{min}^{-1}$ ), the migration of the TCP from the liquid phase to the surface of the *Odorata* particles cannot be the rate-determining step. The experiments were done at pH 5, an optimum pH for the adsorption of TCP by *Odorata*, so it could be assumed that the interaction between the adsorbent and adsorbate occurred instantly. In that regard, the interaction (binding) of TCP with the *Odorata* may not be the rate-limiting stage. Therefore, the rate-determining step could either be the migration of TCP through the *Odorata* particle pores (intra-particle diffusion) or the liquid-film diffusion process. According to Alemayehua et al. (2011) the following equation, which is known as the liquid-film model, can be applied to predict whether liquid-film diffusion is the rate-determining step in an adsorption process:

$$\ln(1-F) = -k_{fd}t \quad (13)$$

where:

- $F$  is a constant ( $F = q_t/q_e$ )
- $k_{fd}$  is the adsorption rate constant
- $t$  is time in min

$$q_t = \frac{(C_o - C_t)v}{w_s} \quad (14)$$

where:

- $C_o$  and  $C_t$  represent the initial concentration and the remaining concentration at different time intervals.

A linear plot of  $-\ln(1-F)$  against  $t$ , passing through the origin (0, 0), indicates that liquid film diffusion is the rate-determining step of the kinetics of the adsorption process. According to Li et al. (2011) and Wang et al. (2011) the following equation can be applied to predict whether intra-particle diffusion if the rate-limiting step in an adsorption process:

$$q_t = K_p t^{1/2} + C \quad (15)$$

where:

- $K_p$  is the intra-particle diffusion rate constant, in  $\text{mg}\cdot\text{g}^{-1}\cdot\text{min}^{1/2}$

When the plot  $q_t$  against  $t^{1/2}$  is linear and passes through the origin (0, 0) then the intra-particle diffusion process is the primary limiting mechanism (Tofighy et al., 2011). Figure 7(a) and Figure 7(b) illustrate the results for liquid-film diffusion and intra-particle diffusion transport models, respectively. Intra-particle diffusion was possible because once the TCP molecules are saturated at the exterior surface of *Odorata*, the TCP molecules can enter the pores of the adsorbent and adsorb on the interior surface of the particles (Hameed et al., 2008). Comparing the results in Figs 7(a) and 7(b), it can be seen that the liquid-film was the rate-determining step. This observation could be due to the hydrophilic nature of the *Odorata* (like most plant materials). Hydrophilic materials tend to interact with water strongly through hydrogen bonding thereby

decelerating the water permeability and this will slow down the rate at which the TCP reaches the adsorbent active sites. In order to check the applicability of rate law, kinetic data were fitted to the pseudo-first order equation and pseudo-second order rate expressions. Investigating kinetics of adsorption experiments is important especially if the experiments are to be scaled up. The pseudo-first order equation is expressed as follows:

$$\ln(q_e - q_t) = \ln(q_e) - \frac{k_1}{2.303} t \quad (16)$$

where:

- $q_e$  and  $q_t$  refer to the amount of TCP ( $\text{mg}\cdot\text{l}^{-1}$ ) adsorbed on the Odorata at equilibrium
- $t$  is time (min)
- $k_1$  is the rate constant ( $\text{min}^{-1}$ )

Plotting  $\ln(q_e - q_t)$  vs.  $t$  should yield a linear graph (shown in Fig. 7(c)) where the experimental equilibrium adsorption capacity  $q_{e, \text{exp}}$  is extrapolated from the y-intercept. The pseudo-second order reaction kinetic model is expressed by the following relation (Doullia et al., 2009):

$$\frac{t}{q_t} = \frac{1}{k_2 q_e^2} + \frac{t}{q_e} \quad (17)$$

where:

- $k_2$  is the second-order rate constant

If second-order kinetics is applicable,  $t/q_t$  should show a linear relationship with  $t$ . The results are shown in Fig. 7(d).

The  $R^2$  corresponding to the pseudo-first order equation was found to be: 0.6638 ( $50 \text{ mg}\cdot\text{l}^{-1}$ ), 0.6565 ( $65 \text{ mg}\cdot\text{l}^{-1}$ ), 0.7113 ( $80 \text{ mg}\cdot\text{l}^{-1}$ ), and 0.7622 ( $100 \text{ mg}\cdot\text{l}^{-1}$ ). The pseudo-second order model had the following  $R^2$ : 0.9932 ( $50 \text{ mg}\cdot\text{l}^{-1}$ ), 0.9827 ( $65 \text{ mg}\cdot\text{l}^{-1}$ ), 0.9775 ( $80 \text{ mg}\cdot\text{l}^{-1}$ ), and 0.9860 ( $100 \text{ mg}\cdot\text{l}^{-1}$ ). Based on the  $R^2$  values, the adsorption of TCP onto Odorata follows the pseudo-second order model. This observation was confirmed by the normalised standard deviation,  $\Delta q(\%)$ , which can be expressed as follows:

$$\Delta q(\%) = 100 \sqrt{\frac{\sum [(q_{e, \text{exp}} - q_{e, \text{cal}}) / q_{e, \text{exp}}]^2}{N - 1}} \quad (18)$$

where:

- $q_{e, \text{exp}}$  and  $q_{e, \text{cal}}$  is the experimental and calculated saturation adsorption amount, respectively
- $N-1$  is the degrees of freedom

The experimental  $q_e$  and the calculated  $q_e$  are summarised in Table 4.

The  $\Delta q(\%)$  obtained for the pseudo-first order kinetic model ranged from 22.02% to 33.21% for TCP initial concentration range used in this study. The  $\Delta q(\%)$  for the pseudo-first order

$C_0$ (mg/l)	$q_{e, \text{exp}}$	pseudo-first order		pseudo-second order	
		$q_{e, \text{cal}}$	$\Delta q(\%)$	$q_{e, \text{cal}}$	$\Delta q(\%)$
100	11.23	14.7	30.9	14	24.67
80	9.046	7.033	22.25	10.67	17.95
65	7.656	5.97	22.02	8.928	16.61
50	6.113	4.083	33.21	6.729	10.08

was relatively higher compared to the  $\Delta q(\%)$  values obtained for the pseudo-second order model. The  $\Delta q(\%)$  corresponding to the pseudo-first order kinetic model ranged from 10.08% to 24.67%. These results confirm that the adsorption of TCP by the table salt treated-Odorata can be described by the pseudo-second order model.

## CONCLUSIONS

This work has shown that the table salt treated-Odorata has potential as an adsorbent for TCP. It has been demonstrated that ANN could be used to simulate the removal of TCP from aqueous media using the table salt treated-Odorata. The following conclusions are drawn from the results of the present work:

- Kinetic batch tests demonstrated that at pH 5, 99% of TCP could be removed from solution given sufficient loading rate and contact time using Odorata treated with table salt.
- Thermodynamic studies showed that the adsorption of TCP by the new adsorbent is thermally feasible and is governed by chemical adsorption mechanism.
- It was established that the experimental data fit the selected adsorption isotherms in the following order: Langmuir > Freundlich > Temkin > D-R.
- Kinetic modelling of removal of phenol was done using the pseudo-first order and pseudo-second order rate expressions. Based on the normalised standard deviation, the pseudo-second order is suitable to describe the adsorption of TCP by Odorata. Further kinetic modelling revealed that liquid-film diffusion is the rate-determining step in the adsorption process.

The advantages of using a plant material in water treatment are low moisture resistance which allows swelling of the fibres, low heat resistance which makes thermal recycling possible, environmentally friendly and easy processing (no wearing of tools and no skin irritation), and low production and investment costs.

## ACKNOWLEDGEMENTS

This work was financially supported by the University of Johannesburg through the Faculty of Science. The authors would like to extend their sincere gratitude to Mr. Thembinkosi Cower Simelane for collecting the *Chromolaena odorata* stems.

## REFERENCES

- AHMARUZZAMAN M (2008) Adsorption of phenolic compounds on low-cost adsorbents: A review. *Adv. Coll. Interf. Sci.* **14** 48–67.
- ALEMAYEHUA E, THIELE-BRUHN S and LENNARTZA B (2011) Adsorption behaviour of Cr(VI) onto macro- and micro-vesicular volcanic rocks from water. *Sep. Purif. Technol.* **78** 55–61.
- ALIX A, PHILIPPE E, BESSADOK A, LEBRUN L, MORVAN C and MARAIS S (2009) Effect of chemical treatments on water sorption and mechanical properties of flax fibres. *Bioresour. Technol.* **100** 4742–4749.
- BYSTRZEJEWSKI M and PYRZYŃSKA K (2011) Kinetics of copper ions sorption onto activated carbon, carbon nanotubes and carbon-encapsulated magnetic nanoparticles. *Coll. Surf. A: Physicochem. Eng. Aspects* **377** 402–408.
- DENIZLI A, CIHANGIR N, TUZMEN N and ALSANCAK G (2005) Removal of chlorophenols from aquatic systems using the dried and dead fungus *Pleurotus sajor caju*. *Bioresour. Technol.* **96** 59–62.
- DLAMINI DS, MISHRA AK and MAMBA BB (2012a) Kinetic and equilibrium studies of the removal of Pb(II) from aqueous solutions



- using Na<sub>2</sub>SO<sub>4</sub>-EVA/Cloisite® 20A composite. *Mater. Chem. Phys.* **133** 369–375.
- DLAMINI DS, MISHRA AK and MAMBA BB (2012b) Adsorption behavior of ethylene vinyl acetate and polycaprolactone-bentonite composites for Pb(II) uptake. *J. Inorg. Organomet. Polym. Mater.* **22** 342–351.
- DLAMINI DS, MISHRA AK and MAMBA BB (2012c) Morphological, transport and adsorption properties of ethylene vinyl acetate-polyurethane/bentonite clay composites. *J. Appl. Polym. Sci.* **124** 4978–4985.
- DOULIA D, LEODOPOULOS C, GIMOUHOPOULOS K and RIGAS F (2009) Adsorption of humic acid on acid-activated Greek Bentonite. *J. Coll. Interf. Sci.* **340** 131–141.
- DUTTA S, PARSONS SA, BHATTACHARJEE C, BANDHYO-PADHYAY S and DATTA S (2010) Development of an artificial neural network model for adsorption and photocatalysis of reactive dye on TiO<sub>2</sub> surface. *Exp. Syst. Appl.* **37** 8634–8638.
- ERRAIS E, DUPLAY J, DARRAGI F, M'RABET I, AUBERT A, HUBER F and MORVAN G (2011) Efficient anionic dye adsorption on natural untreated clay: Kinetic study and thermodynamic parameters. *Desalination* **275** 74–81.
- FAN J, ZHANG J, ZHANG C, REN L and SHI Q (2011) Adsorption of 2, 4, 6-trichlorophenol from aqueous solution onto activated carbon derived from loostrife. *Desalination* **267** 139–146.
- HAMEED BH, TAN IAW and AHMAD AL (2008) Adsorption isotherm, kinetic modeling and mechanism of 2, 4, 6-trichlorophenol on coconut husk-based activated carbon. *Chem. Eng. J.* **144** 235–244.
- HOEK EMV, GHOSH AK, HUANG X, LIONG M and ZINK JI (2011) Physical-chemical properties, separation performance, and fouling resistance of mixed-matrix ultrafiltration membranes. *Desalination* **283** 89–99.
- KARA H, AYYILDIZ FH and TOPKAFI M (2008) Use of amino-phyl silica-immobilized humic acid for Cu(II) ions removal from aqueous solution by using a continuously monitored solid phase extraction technique in a column arrangement. *Coll. Surf. A: Physicochem. Eng. Aspects* **312** 62v72.
- KUMAR NS, WOO H-S and MIN K (2012) Equilibrium and kinetic studies on biosorption of 2, 4, 6-trichlorophenol from aqueous solutions by *Acacia leucocephala* bark. *Coll. Surf. B: Biointerf.* **94** 125–132.
- LI L, LIU F, JING X, LING P and LI A (2011) Displacement mechanism of binary competitive adsorption for aqueous divalent metal ions onto a novel IDA-chelating resin: Isotherm and kinetic modelling. *Water Res.* **45** 1177–1188.
- MAHVI AH, MALEKI A and ESLAMI A (2004) Potential of rice husk and rice husk ash for phenol removal in aqueous system. *Am. J. Appl. Sci.* **1** 321–326.
- MOTSA MM, THWALA JM, MSAGATI TAM and MAMBA BB (2011) The potential of melt-mixed polypropylene-zeolite blends in the removal of heavy metals from aqueous media. *Phys. Chem. Earth* **36** 1178–1188.
- MTHOMBO TS, MISHRA AK, MISHRA SB and MAMBA BB (2011) The adsorption behavior of Cu(II), Pb(II), and Co(II) of ethylene vinyl acetate-clinoptilolite nanocomposites. *J. Appl. Polym. Sci.* **121** 3414–3424.
- PEI Z, SHAN X, LIU T, XIE Y, WEN B, ZHANG S and KHAN SU (2007) Effect of lead on the sorption of 2, 4, 6-trichlorophenol on soil and peat. *Environ. Pollut.* **147** 764–770.
- PUYOL D, MOHEDANO AF, RODRIGUEZ JJ and SANZ JL (2011) Effect of 2, 4, 6-trichlorophenol on the microbial activity of adapted anaerobic granular sludge bioaugmented with *Desulfitobacterium* strains. *New Biotechnol.* **29** 79–89.
- SEN TK and GOMEZ D (2011) Adsorption of zinc (Zn(II)) from aqueous solution on natural Bentonite. *Desalination* **267** 286–294.
- SHIN K-Y, HONG J-Y and JANG J (2010) Heavy metal ion adsorption behavior in nitrogen-doped magnetic carbon nanoparticles: Isotherms and kinetic study. *J. Hazardous Mater.* **190** 36–44.
- SHUKLA A, ZHANG YH, DUBEY P, MARGRAVE JL and SHUKLA SS (2002) The role of sawdust in the removal of unwanted materials from water. *J. Hazardous Mater.* **B95** 137–152.
- SÖLENER M, TUNALI S, ÖZCAN AS and GEDIKBEY AT (2008) Adsorption characteristics of Pb<sup>2+</sup> ions onto the clay/poly (methoxyethyl) acrylamide (PMEA) composite from aqueous solutions. *Desalination* **223** 308–322.
- SUBRAMANI A, HUANG X and HOEK EMV (2009) Direct observation of bacterial deposition onto clean and organic-fouled polyamide membranes. *J. Coll. Interf. Sci.* **336** 13–20.
- SZOPA J, WRÓBEL-KWIATKOWSKA M, KULMA A, ZUK M, SKÓRKOWSKA-TELICHOWSKA K, DYMIŃSKA L, MAĆZKA M, HANUZA J, ZEBROWSKI J and PREISNER M (2009) Chemical composition and molecular structure of fibers from transgenic flax producing polyhydroxybutyrate, and mechanical properties and platelet aggregation of composite materials containing these fibers. *Compos. Sci. Technol.* **69** 2438–2446.
- TAN IAW, AHMAD AL and HAMEED BH (2009) Adsorption isotherms, kinetics, thermodynamics and desorption studies of 2, 4, 6-trichlorophenol on oil palm empty fruit bunch-based activated carbon. *J. Hazardous Mater.* **164** 473–482.
- TURANA NG, MESCIB B and OZGONENEL O (2011) The use of artificial neural networks (ANN) for modeling of adsorption of Cu(II) from industrial leachate by pumice. *Chem. Eng. J.* **171** 1091–1097.
- TOFIGHY MA and MOHAMMADI T (2011) Adsorption of divalent heavy metal ions from water using carbon nanotube sheets. *J. Hazardous Mater.* **185** 140–147.
- WANG XS, LU ZP, MIAO HH, HE W and SHEN HL (2011) Kinetics of Pb (II) adsorption on black carbon derived from wheat residue. *Chem. Eng. J.* **166** 986–993.
- YETILMEZSOY K and DEMIREL S (2008) Artificial neural network (ANN) approach for modeling of Pb(II) adsorption from aqueous solution by Antep pistachio (*Pistacia Vera L.*) shells. *J. Hazardous Mater.* **153** 1288–1300.
- ZAGHOANE-BOUDIAF H and BOUTAHALA M (2011) Adsorption of 2, 4, 5-trichlorophenol by organo-montmorillonites from aqueous solutions: Kinetics and equilibrium studies. *Chem. Eng. J.* **170** 120–126.

## APPENDIX

Supplemental information:

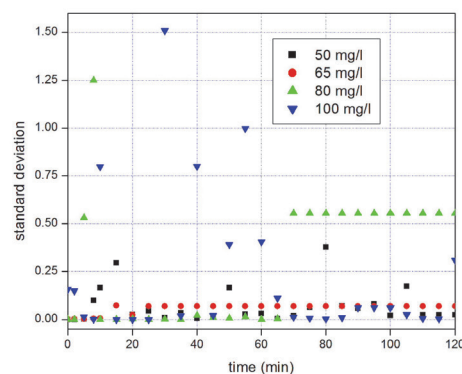


**Figure S1**  
Agreement between real and simulated adsorption efficiency for adsorption of TCP from water by table salt treated-Odorata.

